Thermodynamic Cartography and Structure/Property Mapping of Commercial Platinum Catalysts

A. S. Barnard[a], and L. Y. Chang[b]

[a] *CSIRO Materials Science and Engineering, Clayton, VIC, 3168, Australia.*
[b] *Monash Centre for Electron Microscopy and School of Chemistry, Monash University, Clayton, Australia.*

Supplementary Information

The theoretical calculations were performed from first principles using Density Functional Theory (DFT) within the Generalized Gradient Approximation (GGA), with the exchange-correlation functional of Perdew-Burke-Ernzerhof (PBE) [1]. This was implemented via the Vienna Ab initio Simulation Package (VASP) [2,3] which spans reciprocal space with a plane-wave basis expanded to a given kinetic energy cut-off (in this case 230 eV), and utilizes an iterative self–consistent scheme to solve the Kohn-Sham equations using an optimized charge-density mixing routine. All calculations used Projected Augmented Wave (PAW) potentials [4,5], and were performed to an energy convergence of 10^{-4} eV. Spin polarization was included, and the PAW potentials are generated relativistically (including mass-velocity and Darwin terms), so that the radial wave functions are solutions of the scalar relativistic radial equation (as has previously been the case with similar calculations on gold [6,7]). However, since spin orbit interaction was not included in the all-electron part of the PAW Hamiltonian the spin directions were not coupled to the crystalline structure and the results are not relativistic in this case.

Using this approach, the value of the bulk modulus was calculated to be 276±12 GPa, which is in very good agreement with the value of 309 GPa [8] and 314 GPa [9] calculated using LDA, 246 GPa [9], 241 GPa[10] and 246 GPa [11] calculated using GGA , and the experimental values measured at 278 GPa [12], 283 GPa [13] and 288 GPa [14].

In this paper the surfaces were modelled using periodic slabs generated by cleaving a three dimensional (periodic) supercell along the crystallographic planes of interest, and adding a 15 Å layer of vacuum space. The periodic supercell for the flat and stepped (111) surfaces (shown in figure S1 and S2) contain 108 and 122 atoms, respectively; the periodic supercell for the flat and stepped (100) surfaces (shown in figure S3 and S4) contain 128 and 136 atoms, respectively, and the 1x1 (110) surface contains 144 Pt atoms (as shown in figure S5). In the case of the (100) surface, the step was created via the addition of a partial layer in the terminal planes, as this is consistent with the type of step observed experimentally. In the case of the (111) surface, a step created in this way would introduce both a rise and a fall (effectively two steps per surface) and would not be representative of the experimental system. Therefore, to avoid this problem, and introduce only “rises”, the step on the (111) surfaces has been created by removing half of the terminal layer and rotating the slab around the axis orthogonal to both the surface and the step until the periodicity through the supercell boundaries was recovered (see figure S2).

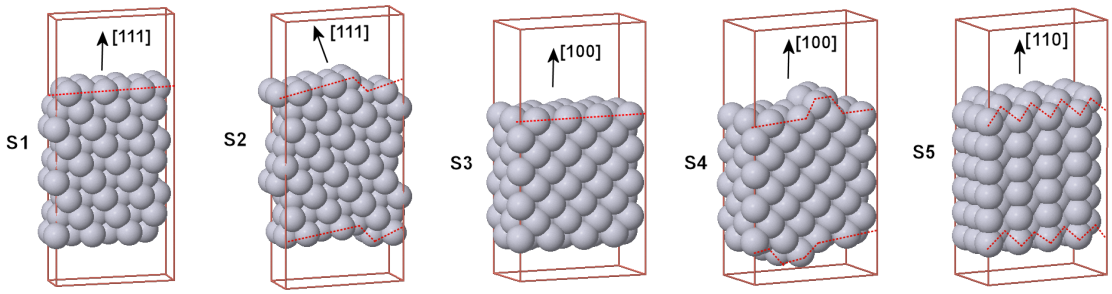

Figure: S1 (left) the 108 atom (111) surface slab, S2 showing the 122 atom stepped (111) surface slab, S3 (left) the 128 atom (100) surface slab, S4 showing the 136 atom stepped (111) surface slab, and S5 (right) showing the 144 atom (110) surface slab. The relaxation was restricted to the 4 terminal layers of the upper and lower surfaces, while the central planes were constrained to the bulk-like positions. The dotted lines are to guide they eyes along the steps.

In each of these structures, the surfaces were fully relaxed by optimizing the atoms in the 4 outer most atomic layers (the terminal plane, and three further planes beneath), which is consistent with the experimental observations. The atomic planes in the center of the slabs were restricted to the bulk-like atomic positions. This has the advantage of providing more surfaces for analysis (both upper and lower facets), will still constraining the bulk like positions far from the surface. The relaxations were performed using an efficient matrix-diagonalization routine based on a sequential band-by-band residual minimization method of single-electron energies [15,16] with direct inversion in the iterative subspace, without symmetry constraints. This methodology has previously been used successfully to model the surfaces of metals [5], and for use in modelling the morphology of metal nanostructures [17,18,19,20].

Based on these simulations the surface energies γ_i (for a surface in orientation i = hkl or hkl,step), can be defined in terms of μ_{Pt}, the chemical potential of bulk FCC platinum as follows:

$$\gamma_i = \frac{1}{2A_i}\left[E_i(N) - N\mu_{Pt} + P\Delta V - T\Delta S\right]$$

where $E_i(N)$ is the total energy of a fully relaxed surface slab in orientation i (containing N platinum atoms), A_i is the explicit area of the supercell in the plane of the surface, P is the pressure, ΔV is the volume change due to surface relaxation, T is the temperature and ΔS is entropy change which is normally dominated by the vibrational entropy from phonons. Since all of the simulations were performed here at low temperature (and extrapolated to $T = 0\mathrm{K}$), the second term is zero. The entropic contributions must be added empirically, as described in the main text, and rigorously validated in reference 7. Furthermore, although surface reconstructions were observed, the second last term will be disregarded, as inaccuracies introduced by the omission will be less than the uncertainties inherent in the DFT calculations.

Using this technique, the surface energy was calculated for all of the low index surfaces of interest. The isotropic surface stresses were computed from the trace of the surface stress tensor, which is output directly by the VASP code. These results are provided below in Table 1, along with simular results obtained by others, for the purposes of comparison. There are numerical difference between the results obtained by different studies, due usually to different DFT approximation, exchange correlations functional, meshes sizes and convergence criteria, but we see that in cases where authors have treated more than one surface or value, the relative values are (for the most part) consistent among the different sets.

Table 1: Surface energies γ_{hkl} and $\gamma_{hkl,step}$, and isotropic surface stresses σ_{hkl} and $\sigma_{hkl,step}$, for the relevant low index surface of platinum, reported by various research studies.

Source (Method)	γ_{111}	$\gamma_{111,step}$	γ_{100}	$\gamma_{100,step}$	γ_{110}	σ_{111}	$\sigma_{111,step}$	σ_{100}	$\sigma_{100,step}$	σ_{110}
This Study (DFT, GGA)	1.26	1.33	1.72	1.77	1.78	5.41	5.87	3.40	2.91	2.01
Reference 8 (DFT, LDA)	2.19					5.61				
Reference 9 (DFT, GGA)						6.04				2.09*
Reference 9 (DFT, LDA)						6.34				2.95*
Reference 21 (DFT, GGA)	1.35					5.61				
Reference 22 (DFT, GGA)	1.49		1.85			4.25		3.32		
Reference 23 (DFT, GGA)	1.49		1.81		1.85					
Reference 24 (DFT, LDA)	1.99					4.01				
Reference 24 (DFT, GGA)	1.55					3.52				
Reference 25 (DFT)	2.15		2.72							
Reference 26 (Experiment†)						4.9				
Reference 27 (Experiment)	2.49									

* Averaged over in-plane directions.

† Grazing incidence X-ray diffraction

However, since the intention here is to use these values to determined the shape of nanoparticles enclosed by these surfaces (see Main Text), it is the relative values that are important, and so it is imperative that a consistent set of values is calculated using the same method.

Supplementary Information - Reference

1 J. P. Perdew, K. Burke, M. Ernzerhof, Phys. Rev. Lett. 77, 3865 (1996).

2 G. Kresse, J. Hafner, Phys. Rev. B, 47, RC558 (1993).

3 G. Kresse, J. Furthmüller, Phys. Rev. B, 54, 11169 (1996).

4 P. E. Blöchl, Phys. Rev. B, 50, 17953 (1994).

5 G. Kresse, D. Joubert, Phys. Rev. B, 59, 1758 (1999).

6 A. S. Barnard, X. M. Lin, L. A. Curtiss, J. Phys. Chem. B 109, 24465 (2005).

7 A. S. Barnard, N. Young, A. I. Kirkland, M. A. van Huis, H. Xu, ACS Nano 3, 1431 (2009).

8 R. J. Needs, M. Mansfield, J. Phys.: Condens. Matter, 1, 7555, (1989).

9 M. Blanco-Rey, S. J. Jenkins, J. Phys.: Condens. Matter, 22, 135007 (2010).

10 J. L. F. Da Silva, C. Stampfl, M. Scheffler, Surf. Sci. 600, 703 (2006).

11 A. Khein, D.J. Singh, C.J. Umrigar, Phys. Rev. B 51, 4105 (1995).

12 C. Kittel, *Introduction to Solid State Physics* 5th Edn, Wiley, New York (1976)

13 D. R. Lide (ed) 2009 *CRC Handbook of Chemistry and Physics* 90th edn. (Boca Raton, FL: CRC Press)

[14] R. E. Macfarlane, J. A. Rayne, C. K. Jones, Phys. Lett. 18, 91 (1965)
[15] G. Kresse J. Furthmüller, Comp. Mat. Sci. 6, 15 (1996).
[16] D.M. Wood, A. Zunger, J. Phys. A, 18, 1343 (1985).
[17] A. S. Barnard, L. A. Curtiss, ChemPhysChem, 7, 1544 (2006).
[18] A. S. Barnard, J. Phys. Chem. B, 110, 24498 (2006).
[19] A. S. Barnard, L. A. Curtiss, J. Mater. Chem. 17, 3315 (2007).
[20] A. S. Barnard, J. Phys. Chem. C 112, 1385 (2008).
[21] Ž. Crljen, D. Šokčević, R. Brako, P. Lazić, Vacuum 71, 101 (2003).
[22] V. Zólyomi, L. Vitos, S. K. Kwon, J. Kollár, J. Phys.: Condens. Matter 21, 095007 (2009).
[23] N. E. Singh-Miller, N. Marzari, Phys. Rev. B 80, 235407 (2009).
[24] G. Boisvert, L. J. Lewis, M. Scheffler, Phys. Rev. B, 57, 1881 (1998)
[25] A. Jaafar, C. Goyhenex, Sol. State Sci. 12, 172 (2010)
[26] G. Prévot, L. Barbier, P. Steadman, Surf. Sci. 604, 1265 (2010)
[27] W. R. Tyson, W. A. Miller, Surf. Sci. 62, 267 (1977).